MCL-1 promiscuity and the structural resilience of its binding partners

Heckmeier, Philipp J ; Ruf, Jeannette ; Janković, Brankica G ; Hamm, Peter

MCL-1 promiscuity and the structural resilience of its binding partners

View Online   Export Citation   CrossMark

Philipp J. Heckmeier,[a] (ID) Jeannette Ruf, (ID) Brankica G. Janković, (ID) and Peter Hamm (ID)

AFFILIATIONS

Department of Chemistry, University of Zurich, Zurich, Switzerland

Note: This paper is part of the JCP Special Topic on New Views of Allostery.
[a]Author to whom correspondence should be addressed: philipp.heckmeier@chem.uzh.ch

ABSTRACT

The allosteric protein MCL-1 and its natural inhibitors, the BH3-only proteins PUMA, BIM, and NOXA regulate apoptosis by interacting promiscuously within an entangled binding network. Little is known about the transient processes and dynamic conformational fluctuations that are the basis for the formation and stability of the MCL-1/BH3-only complex. In this study, we designed photoswitchable versions of MCL-1/PUMA and MCL-1/NOXA, and investigated the protein response after an ultrafast photo-perturbation with transient infrared spectroscopy. We observed partial α-helical unfolding in all cases, albeit on strongly varying timescales (1.6 ns for PUMA, 9.7 ns for the previously studied BIM, and 85 ns for NOXA). These differences are interpreted as a BH3-only-specific "structural resilience" to defy the perturbation while remaining in MCL-1's binding pocket. Thus, the presented insights could help to better understand the differences between PUMA, BIM, and NOXA, the promiscuity of MCL-1, in general, and the role of the proteins in the apoptotic network.

16 January 2024 11:26:02

I. INTRODUCTION

Protein–protein interactions are the fundamental driving force for a majority of cellular processes.[1,2] Understanding the molecular mechanisms behind this protein–protein interplay is of highest scientific interest.[3] For numerous protein complexes, it is not clear how they form, how small conformation fluctuations contribute to the complex function and stability, and whether there are intertwined intermediate states of altered conformation.[4,5] Illuminating the nuances of these dynamic processes is particularly essential for complexes formed by intrinsically disordered proteins.[6] These proteins do not assume an ordered structure in their isolated form but only when they are bound to their complex partner. For intrinsically disordered proteins, the process of complex formation can be explained with models,[7,8] such as the induced fit model,[9] the conformational selection model,[4] or a hybrid version of both theories.[10] Intrinsic disorder plays a significant role in promiscuous protein networks, as it enables the complex formation with numerous binding partners.[11,12] Being on "the edge of chaos"[13] ensures structural and functional flexibility and provides an ideal basis for diverse protein–protein interactions, for instance, in a network of activator, inhibitor, and effector proteins.

The BCL-2 protein family is a paramount example for an intricate protein network, which is driven by promiscuous interactions of several intrinsically disordered protein domains. In this protein family, categorized in subfamilies based on the type and the number of their BCL-2 homology (BH) domains, the disordered binding domains of so-called BH3-only proteins—they solely have a BH3 domain—form complexes with numerous other BCL-2 proteins, thereby controlling apoptosis in a finely balanced manner.[14–17] The BH3-only proteins, abundant when cells suffer cytotoxic stress,[18–20] either directly activate the pro-apoptotic effector proteins (BAK and BAX) or inhibit the anti-apoptotic effector-inhibitors, such as the Myeloid Cell Leukemia 1 (MCL-1) protein, one of the key players in apoptosis regulation[15] (Fig. 1). MCL-1 is overexpressed in various tumor variants, which makes it of high interest in therapeutic application.[18,21–25] In the past, MCL-1 was demonstrated to exhibit allosteric signaling between the canonical binding pocket and remote parts of the protein.[26] The time scales of this allosteric communication are putatively in the nanosecond time regime.[27] At its canonical binding site, MCL-1 promiscuously binds the α-helical binding domain of the BH3-only proteins PUMA, BIM, and NOXA,[28,29] most likely by induced fit.[30–34]
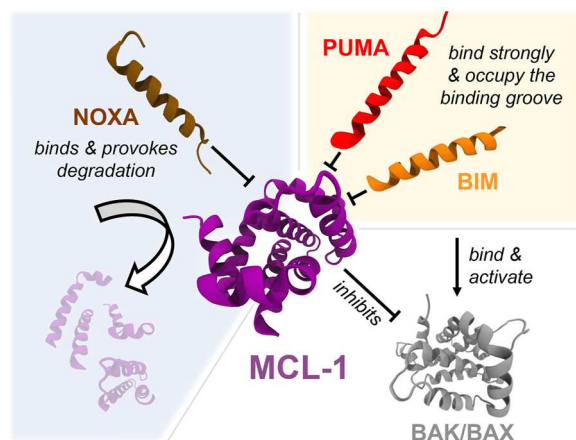
FIG. 1. The protein MCL-1 promiscuously binds BH3-only peptides NOXA, PUMA, and BIM and has a central position in an entangled binding network, regulating apoptotic effector proteins BAK and BAX.

PUMA and BIM inhibit MCL-1 by occupying its binding pocket with affinities in the sub-nanomolar range, but additionally bind other anti-apoptotic factors and the pro-apoptotic effector proteins BAK and BAX.[17,28,35] In contrast, NOXA binds MCL-1 specifically and with a weaker affinity, however, affects the degradation of the whole complex.[36]

In their intriguing review,[15] Kale *et al.* describe this interplay of different pro- and anti-apoptotic factors very figuratively as a "dance" of various partners—an interesting and vivid depiction of protein promiscuity. In this "apoptotic dance," the protein affinity and stability determine the complex formation and whether cell death will be initiated or not.

To date, little is known about the protein dynamics behind the MCL-1/BH3-only complex stability and formation, let alone intermediate states of BH3-only folding and unfolding at MCL-1's binding groove.[37] Investigating subtle, dynamical rearrangements inside proteins like the MCL-1/BH3-only complex is connected to a fundamental challenge: the ability to resolve structural flexibility and small conformational fluctuations in a reasonable time frame.[38,39] In the past, the dynamics of protein ensembles—intrinsically disordered or folded—have been experimentally studied via single-molecule FRET spectroscopy,[40,41] NMR spectroscopy,[42,43] as well as transient infrared (IR) spectroscopy.[44,45] IR spectroscopy allows the differentiation of very small conformational differences[46] and, in its transient form, the sensitive detection of non-equilibrium processes,[47] making it a highly suitable method to study MCL-1/BH3-only complexes.

To selectively trigger a dynamical process inside a protein for transient IR spectroscopy, a fast and precisely induced perturbation of the proteins is required, ideally initiated by short light pulses. In this regard, a plethora of photoreceptor proteins, i.e., light-sensitive or fluorescent, have been investigated in the past.[48–54] Beyond proteins that show natural photo-activity, linking azobenzene photoswitches covalently to selected protein domains—most prominently α-helical structures—defines a potent strategy to introduce photo-sensitivity in molecules, which are otherwise "blind" to

light. The light-induced isomerization of the cross-linked azobenzene moiety leads to a fast perturbation of the secondary structure,[55] and in turn to a slower protein response, both of which can be detected via transient IR spectroscopy.[56–58] With this technique, the allosteric signal propagation in PDZ domains and the unbinding in the RNase S complex were investigated.[44,45,59] Similarly, we recently revealed the signal propagation inside the MCL-1/BIM complex, indicating that the structural adaptations of MCL-1 upon photo-perturbation may be classified as an allosteric communication.[34]

In this study, we apply transient IR spectroscopy to explore the protein dynamics of the intrinsically disordered binding domains of PUMA and NOXA in complex with MCL-1. An azobenzene photoswitch has been covalently linked to the short PUMA and NOXA peptides. The induced isomerization of the photoswitch leads to a subsequent destabilization of the secondary structure of the linked peptides, yet remaining bound to MCL-1 (Fig. 2). Together with data from the previously analyzed MCL-1/BIM complex,[34] we classify the kinetic response of these three MCL-1/BH3-only complexes and discuss how the observed protein dynamics integrate into the promiscuous nature of the MCL-1/BH3-only system.
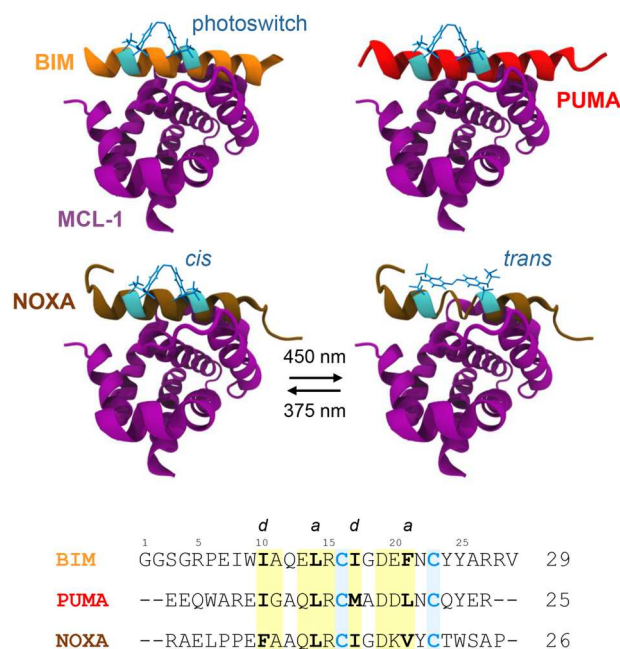
FIG. 2. Structures of MCL-1 (purple) binding BIM (orange), PUMA (red), or NOXA (brown), adapted from PDB entries 2NL9,[28] 2ROC,[29] and 2ROD,[29] respectively. The peptides were covalently crosslinked with an azobenzene photoswitch (blue) at introduced Cys residues (cyan). Illumination with 450 nm light promotes the isomerization of the photoswitch from the *cis*-state to the *trans*-state, exemplified here for NOXA. The opposite direction can be induced with 375 nm light. The α-helical BH3-only peptides are destabilized in the *trans*-state. Aligned peptide sequences are also shown together with the *a* and *d* positions of their heptad pattern. The residue positions that are known to form the contact interface with the binding groove of MCL-1 are marked in yellow.[60]

16 January 2024 11:26:02

II. RESULTS

A. Complex design

We designed photoswitchable variants of the binding domains of PUMA and NOXA in complex with MCL-1 to compare them to the previously generated photoswitchable MCL-1/BIM variant.[34] The domains, from here on *pars-pro-toto* referred to as PUMA, NOXA, and BIM, are 25 to 29 amino acid long intrinsically disordered peptides that become α-helical when complexing with MCL-1.[16] They interact with a classical heptad pattern with hydrophobic side chains at the a/d positions of the helix (Fig. 2, sequences). On the solvent-exposed side of PUMA and NOXA, we introduced two cysteine residues, which were used to covalently bind the photoswitch 3,3′-bis(sulfonato)-4,4′-bis-(chloroacetamido) azobenzene (BSBCA)[61] to the peptide. In a previous study with BIM, we identified positions 16 and 23 (two consecutive c positions of the heptad pattern) as anchoring points for the azobenzene moiety. For the newly generated complexes, we introduced cysteines at the corresponding positions (Fig. 2, in cyan).

Circular Dichroism (CD) spectroscopy of the isolated BH3-only peptides reveal a random coil structure in both the *cis*-state

and the *trans*-state of the photoswitch [exemplified for PUMA in Fig. 3(a), red and blue]. The CD spectrum of MCL-1 alone displays the classical response for an α-helical structure [Fig. 3(a), black]. When the BH3-only peptides BIM, PUMA, and NOXA are added in equivalent amounts in the dark, in which case the photoswitch is in the *trans*-state [Fig. 3(a), purple], the mean residue ellipticity representing the α-helical content is only slightly divergent from that for MCL-1 alone [Fig. 3(b)]. This proves that the photoswitchable BH3-only peptides assumes an α-helical structure in the presence of their natural binding partner MCL-1. By illuminating the MCL-1/BH3-only complexes with 375 nm laser light, we uniformly switched the photoswitchable BH3-only peptides to the *cis*-state and could detect a small increase in α-helical content for NOXA, PUMA, and BIM [see Fig. 3(b)], as anticipated from the spacing of seven amino acids between the two anchoring points of the photoswitch. Previous results on the photoswitchable MCL-1/BIM complex showed that the dissociation constants in the *cis*- and *trans*-state (<4 μM) fall far below the concentration that we applied in the spectroscopic experiments (>400 μM). For MCL-1/BH3-only complexes, the slight destabilization of the α-helix in the *trans*-state is not sufficient to result in an unbinding event for the concentration range needed in IR spectroscopy.[34]
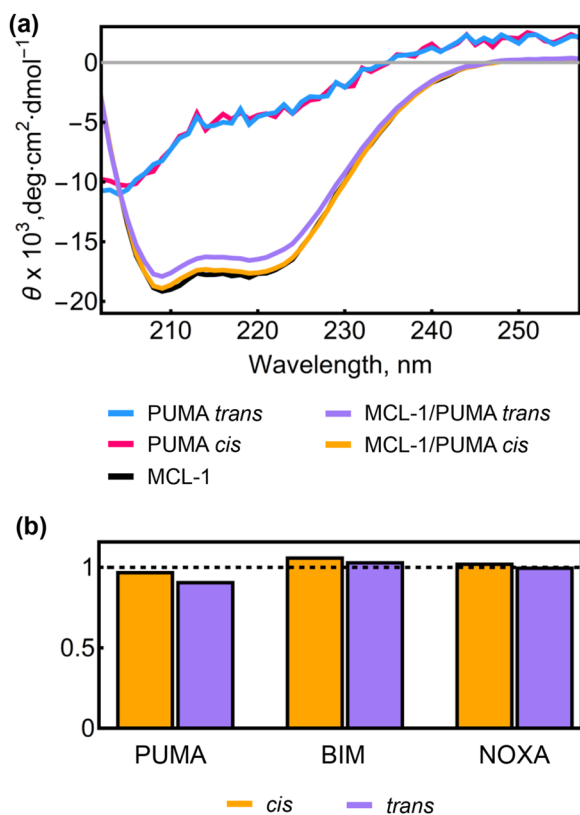
B. Transient IR spectroscopy

For the transient IR experiments, the sample was first prepared in the *cis*-state with the help of a cw-LED at 375 nm. Upon subsequent switching of the azobenzene moiety from the *cis*-state to the *trans*-state by the irradiation with an ultrashort UV/VIS laser pulse at 420 nm, the abrupt isomerization process perturbs the secondary structure of the peptide, and in consequence also that of its binding partner MCL-1. To monitor these structural changes, we set our focus on the C=O stretch vibrations of the protein backbone, i.e., the amide I band in the region around 1650 cm⁻¹. The amide I band serves as an indicator for rearrangements and alterations in the protein structure.[62] We performed these experiments both in a steady-state manner with the help of a Bruker Tensor 27 FTIR spectrometer [Figs. 4(a) and 4(c)], as well as transiently with the pump-probe delay time ranging from picoseconds to 42 μs [Figs. 4(b) and 4(d)]. Additionally, we recorded equivalent steady-state difference spectra of the isolated peptides (Fig. S1). The late time (42 μs) transient spectra are in essence the same as the steady-state difference spectra [Figs. 4(a) and 4(c) red vs black lines], indicating that most of the structural changes have already found their end at this time point.

In order to extract the dynamical processes contained in the transient spectra, we performed global multiexponential fitting, assuming interconverting discrete states with time-invariant spectra,[63–65]

$$d(\omega_i, t_j) = a_0(\omega_i) + \sum_k a(\omega_i, \tau_k) e^{-t_j/\tau_k}. \qquad (1)$$

Here, we treated the amplitudes $a(\omega_i, \tau_k)$, as well as a common set of time constants τ_k as the free fitting parameters, with the number n of exponential terms being restrained to a minimum.[49,66] To find this minimum, we compared the residuals for an increasing number of exponential terms. The absolute values of the residuals decrease with increasing number of terms for $n \le 3$ (PUMA) and for $n \le 2$

FIG. 3. (a) CD spectra of MCL-1 and PUMA (both 20 μM) in isolation and when forming a complex. The PUMA spectra are shown for both the *cis*- and the *trans*-state of the photoswitch. The mean residue ellipticity θ is given to facilitate the secondary structure comparison. (b) Mean residue ellipticity at 220 nm of the MCL-1/peptide complexes relative to that of MCL-1 without peptide (dashed line). The data for BIM are adapted from Heckmeier *et al.*[34]
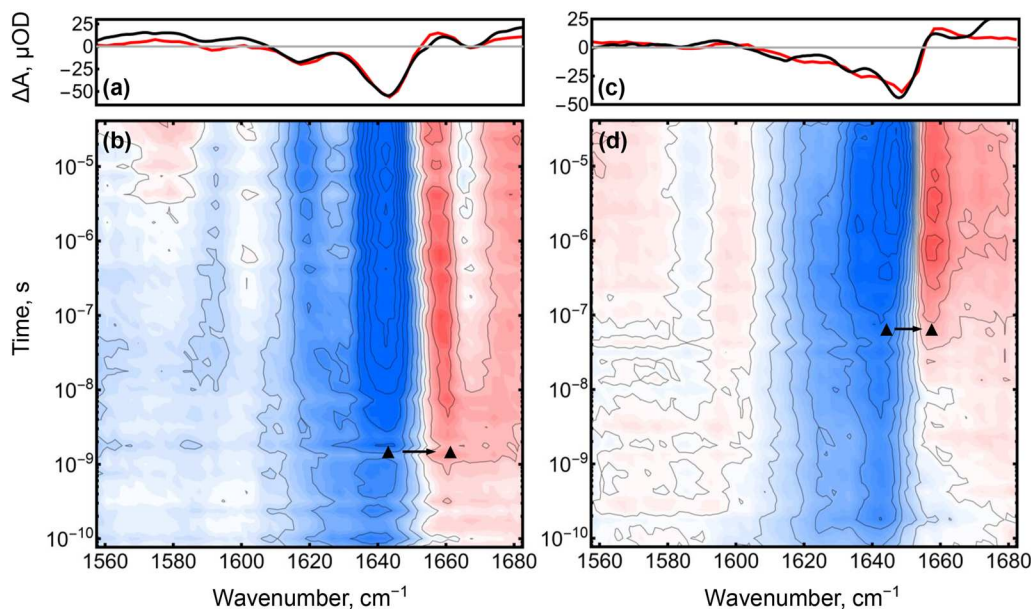
FIG. 4. IR spectroscopic analysis of PUMA [(a) and (b)] and NOXA [(c) and (d)] in complex with MCL-1. [(a) and (c)] Steady-state *cis*-to-*trans* difference spectrum (black) and the last kinetic trace at 42 μs (red). [(b) and (d)] Transient *cis*-to-*trans* difference spectra as a function of pump–probe delay time. The triangles mark the blue shift of the amide I band from $\approx$1640 cm^{-1} to $\approx$1660 cm^{-1}.

(NOXA). For *n* above these thresholds, there were no evident differences anymore. In consequence, the minimal number of terms for PUMA was 3, and for NOXA 2. We fitted the experimental data of PUMA with four states, S$_1$, S$_2$, S$_3$, and a terminal state S$_t$ and three time constants connecting them (τ_{12} = 1.6 ns, τ_{23} = 18 ns, and τ_t = 1.6 μs). For NOXA, three states S$_1$, S$_2$, and S$_t$ and two time constants were sufficient (τ_{12} = 85 ns and τ_t = 1.4 μs). The corresponding
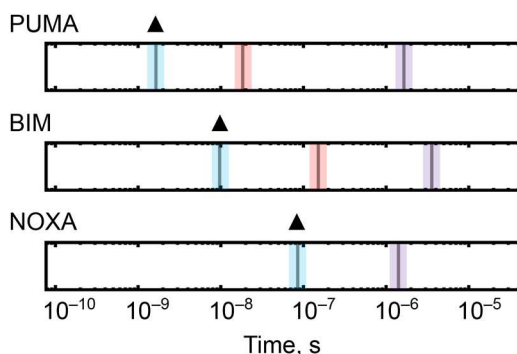

FIG. 5. Timescales of dynamical activity for MCL-1/PUMA, MCL-1/BIM, and MCL-1/NOXA upon photo-perturbation. For PUMA and NOXA, the time constants were determined from the transient spectra in Fig. 4, while the data for BIM were taken from Heckmeier *et al.*[34] Time constant τ_{12}, associated with the spectral blue shift (and thus marked by triangles), is underlined in blue, time constant τ_{23} in red, and the terminal time constant τ_t in purple. For NOXA, τ_{23} cannot be resolved. In Heckmeier *et al.*,[34] we reported an additional time constant prior to 100 ps, which however was related to the pump–pulse duration and hence does not reflect a kinetic process.

time constants in BIM are τ_{12} = 9.7 ns, τ_{23} = 150 ns, and τ_t = 3.6 μs (see Ref. 34).

The observed timescales are summarized in Fig. 5. While the last timescale (τ_t) is more or less the same in all three samples, the preceding two processes (τ_{12} and τ_{23}) vary by almost a factor 100, with PUMA being the fastest and NOXA the slowest. In the case of NOXA, τ_{23} is not resolved, presumably since it coincides with the terminal process τ_t leading to a spectral signature in state S$_t$ that is very similar to those observed for PUMA and BIM.

Assuming a sequential, unidirectional process (see Fig. 6, top), we also calculated evolution associated difference spectra (EADS) according to

$$d(\omega_i, t_j) = \sum_k C_k(t_j) A_k(\omega_i), \qquad (2)$$

where $C_k(t_j)$ is the concentration profile of component k as a function of time t_j, and $A_k(\omega_i)$ its spectrum at probe frequency ω_i. The spectra $A_k(\omega_i)$ are a linear combination of the fitting amplitudes $a(\omega_i, \tau_k)$.[66]

For all investigated peptides, the first EADS, revealing the response immediately after the pump pulse is over, shows in essence a bleach of the amide I band (Fig. 6, red). The subsequent state (Fig. 6, yellow), populated with time constant τ_{12}, reveals an additional positive band on the higher-frequency side, and hence a blue-shift of the amide I band. This blue shift has been similarly detected for MCL-1/BIM[34] and other α-helical peptides[46,67] where it displayed the same asymmetric appearance and was interpreted as a partial α-helical unfolding. The asymmetry in signal strength between the bleach at 1640 cm^{-1} and the emerging feature at 1660 cm^{-1} follows the same trend as already seen for the mentioned
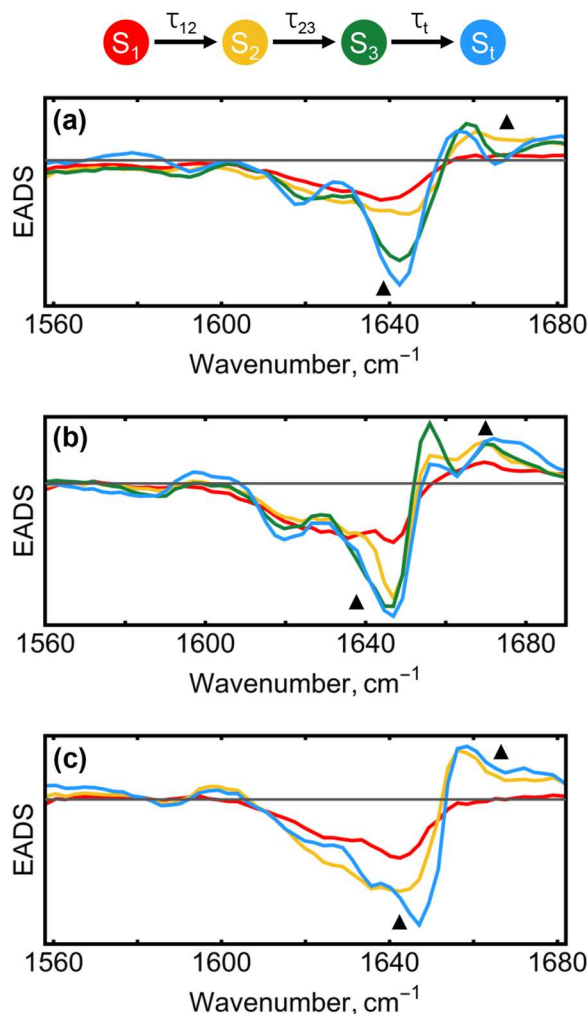
FIG. 6. Evolution associated difference spectra (EADS) of photo-perturbed (a) MCL-1/PUMA, (b) MCL-1/BIM (adapted from a previous study[34]), and (c) MCL-1/NOXA. The triangles mark the blue shift of the amide I band from ≈ 1640 cm^{-1} to ≈ 1660 cm^{-1}.

III. DISCUSSION

MCL-1 promiscuously binds to numerous intrinsically disordered inhibitors, BH3-only peptides, at its binding groove.[28,29] MCL-1's centrality in the cancer-related apoptotic networks and its promiscuous nature makes it of high interest for biochemical and pharmaceutical research.[21,22] In this study, we characterized the promiscuity of MCL-1 on an atomistic level. To that end, we explored the protein response of MCL-1/PUMA and MCL-1/NOXA upon ultrafast photo-perturbation. Together with the recently published data on a photoswitchable MCL-1/BIM variant, we could draw on dynamical information for three of MCL-1's natural inhibitors in a picosecond to microsecond time window.

After the abrupt photo-isomerization of the azobenzene moiety, the three complexes reveal very similar spectroscopic responses, both regarding the late time (steady-state) response [Figs. 4(a) and 4(b)], as well as that of the transient intermediates (Fig. 6). There is, however, one crucial difference between the three investigated MCL-1/BH3-only complexes: Partial α-helical unfolding, occurring with τ_{12}, happens at strongly divergent time points for every BH3-only peptide; see blue lines in Fig. 5. The fastest response was detected for PUMA ($\tau_{12} = 1.6$ ns), succeeded by BIM ($\tau_{12} = 9.7$ ns), and finally by NOXA ($\tau_{12} = 85$ ns). Interestingly, the time point of partial α-helical unfolding does not correlate with the binding affinity of the peptide,[17] but significantly with computed scores for its polarity[68] and hydropathicity,[69] as well as with the decline of α-helical content due to photoswitching (Fig. 7). The latter was determined by measuring triplicates of photoswitchable MCL-1/BH3-only complexes with CD spectroscopy. The stronger the decrease in α-helicity is upon *cis*-to-*trans* isomerization, the faster is its response. The same is true for increasing hydrophilicity as well as polarity.

Disrupting PUMA, which reveals the fastest response, with the *trans*-state azobenzene moiety may result in unfavorable contacts between hydrophilic side chains of PUMA and the hydrophobic interface of the binding groove of MCL-1. This strong tension could be dissolved by a rapid partial α-helical unfolding. Interestingly, a computational study solely on PUMA highlighted the increased α-helical propensity at the C-terminal relative to the rest of the peptide,[70] the same region that we destabilize in our experiments. Apparently, the perturbation of this region, which is innately more likely to form ordered structures, leads to conformational tension and thus to the fast protein response. In contrast, the slow opponent NOXA—inherently more hydrophobic and less polar—is not confronted with comparable tensions; thus, it is not forced to rearrange quickly and, thus, unfolds later. The discrepancies between the peptides may also arise from breaking peptide-exclusive electrostatic interactions at the putative contact interface (Fig. 2, yellow residues) upon photoswitching. Electrostatic interactions at the contact interface are known to support the complex formation of MCL-1 and BH3-only peptides, namely, those formed by MCL-1 Lys234 and Glu9 of NOXA or PUMA (numbering according to the alignment in Fig. 2),[28,71] MCL-1 Asp256/peptide Arg15,[71,72] and MCL-1 Arg263/peptide Asp19.[71,72]

Beyond this atomistic view on the investigated MCL-1/BH3-only complex, we tried to infer the consequences that our observations have for the biological understanding of the system.

systems[34,46,67] and only allows a qualitative rather than a quantitative classification. In Ref. 34, we had also investigated the response a localized vibrational mode directly associated with the photoswitch, supporting this interpretation. The blue-shift can be identified in the raw data of Fig. 4 as well, where it is marked with triangles. While the blue-shifted band is observed for all three samples with very similar spectroscopic characteristics, the timescale with which it appears, τ_{12}, varies by almost a factor 100.

Based on isotope labeling experiments,[34] the subsequent spectral changes occurring with τ_{23} and τ_t have been attributed to mostly the protein MCL-1 responding to the structural perturbation of its binding partner together with further rearrangements of BIM, located inside MCL-1's binding pocket. Based on an analogous spectral signatures, we assume the same for PUMA and NOXA.
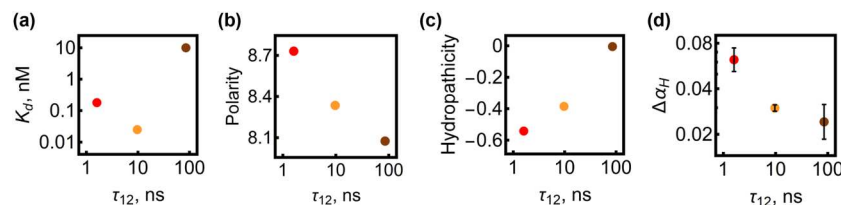
FIG. 7. Correlation of (a) the binding affinity of the peptide, (b) its polarity,[68] (c) its hydropathicity,[69] and (d) the loss in α-helicity upon photoswitching (*cis*-to-*trans*) against time constant τ_{12} for PUMA (red), BIM (orange), and NOXA (brown). The K_d values were taken from Dahal *et al.*,[17] the scores in (b) and (c) were computed from amino acid sequences (see "Methods" for details), and the data points in (d) from CD spectroscopic measurements (see Fig. 3; PUMA: 0.062 ± 0.012; BIM: 0.030 ± 0.001; NOXA: 0.024 ± 0.007; mean $\pm$ standard deviation, n = 3).

First, we note that the observed time constants for the α-helix destabilization match the time scales of putative allosteric communication in MCL-1.[27] This implies that the destabilization of BH3-only domains in the binding pocket of MCL-1 could temporally interfere with synchronous signaling pathways inside MCL-1, making our observation relevant to understand the simultaneity of processes in MCL-1's "apoptotic dance"[15] with its pro-apoptotic inhibitors.

Second, our observations pose the question of how the peptide-specific differences correlate with the promiscuous nature of the MCL-1/BH3-only complexes on a cellular level. Pro-apoptotic BH3-only proteins are "damage sensors" and abundantly expressed when cells suffer cytotoxic stress.[18–20] Although their binding domains share the same α-helical structure of similar length and identical hydrophobic heptad pattern, as well as the same binding site at MCL-1, BH3-only proteins differ substantially in their relationship inside the BCL-2 family and their interaction pattern (Fig. 1). BIM and PUMA bind the full spectrum of the anti-apoptotic BCL-2 family, and also activate the effector proteins BAK and BAX, whereas NOXA selectively inhibits MCL-1 and BCL-2, another member of the same protein family.[15] BIM and PUMA stabilize MCL-1, while NOXA promotes its degradation.[28,36] At this point, we cannot decide whether these functional differences result from structural alterations at the binding groove or from a more complex involvement of other domains that were not investigated in the present study.

Studies with truncated or mutated versions of NOXA demonstrated that the C-terminal region of the binding domain regulates the stability of the MCL-1/NOXA complex and therefore is important to control MCL-1/NOXA degradation[28,36,73] (Fig. 1, left). In *in vivo* experiments with the full size NOXA protein and MCL-1, Willis *et al.* proved that mutating only three residues of the binding domain (alignment position 14, 17, and 21 in Fig. 2) was enough to drastically reduce the biological activity of the full size NOXA protein.[36] The perturbation in our experiments aims precisely at this region of NOXA's binding domain, where apparently subtle differences can entail the dissociation of the protein complex. To maintain its biological function, this region of NOXA has to bind to MCL-1, which requires a certain "structural resilience" for this region, even when the whole complex is destabilized in the proteolytic process. We delimit this "structural resilience" from the already established terms "stability"[74] and "structural plasticity".[75] The former is classically used in a thermodynamic context to describe how partners in a protein complex form and maintain folded conformations.[74,76–78] The latter is frequently used to characterize the ability of promis-

cuous proteins, e.g., BCL-2-type,[79] chaperones,[80,81] trypsin,[82] or protein kinases,[83] to flexibly bind various, different binding partners at the same interface. With "structural resilience," we have in mind a kinetic stabilization, to contrast to a thermodynamics one.

Our results show that even after photo-induced destabilization, the photo-perturbed C-terminus of the NOXA peptide remains folded more than 10 times longer than the equivalent region in other peptides (Fig. 5). While that is definitely speculative, the high structural resilience of NOXA's C-terminus inside the binding pocket of MCL-1 could help to remain in place, even when the whole complex is confronted with major rearrangements leading to the potent proteolysis of MCL-1. Future experiments could test this hypothesis by connecting a mutational analysis of NOXA and *in vivo* screening of MCL-1 proteolysis with monitoring the peptide's structural resilience by IR spectroscopy.

Different to NOXA, PUMA and BIM increase the stability of MCL-1[28,35] and block the binding groove of MCL-1 (Fig. 1, right). This in turn limits MCL-1's ability to bind the effector proteins BAK and BAX. The competition between BIM, PUMA, and the effector proteins for MCL-1 manifests in the extremely high affinities of BIM (K_D = 25 pM) and PUMA (K_D = 180 pM) in comparison to the already high affinities for the effector proteins BAK (K_D = 1.4 nM) and BAX (K_D = 22 nM).[17] Transient IR spectroscopy demonstrated that the structural resilience of PUMA and BIM is smaller than that of NOXA, presumably because their natural role is different, binding the partner in a highly stable complex with little structural flexibility. Any disturbance seems to result in a fast adaptation, i.e., the partial unfolding that we observed in our experiments.

In summary, our study reveals insights into the promiscuity of the anti-apoptotic, allosteric MCL-1 for the intrinsically disordered binding domains of BH3-only proteins. By using transient IR spectroscopy in combination with photo-switchable protein complexes, we quantified the dynamic response of BIM, PUMA, and NOXA in the binding pocket of MCL-1 upon photo-perturbation. All peptides show partial α-helical unfolding, however, on very different timescales. The correlations in Fig. 7 are indicating that the speed of protein response in our system is coupled to the extent of structural rearrangements [Fig. 7(d)] and possibly linked to favorable or unfavorable interactions, caused by the perturbation. Computational studies could test this hypothesis.

NOXA is structurally more resilient than BIM and PUMA. This finding reveals a new viewpoint on the nature of BH3-only peptides, which could help to better understand promiscuous protein–protein

interactions, in general, as well as the design of novel molecules and peptides to therapeutically manipulate the oncologically relevant MCL-1/BH3-only complex.

IV. MATERIALS AND METHODS

A. Peptide preparation

The BH3 domains of PUMA (EEQWAREIGAQLRCMADDL-NCQYER) and NOXA (RAELPPEFAAQLRCIGDKVYCTWSAP), both containing cysteine mutations with a spacing of seven amino acids, were synthesized using solid state peptide synthesis on a Liberty 1 peptide synthesizer (CEM Corporation, Matthews, NC, USA). These peptides were purified analogously to the BIM variant (GGSGRPEIWIAQELRCIGDEFNCYYARRV), which was investigated in a preceding study.[34] The water-soluble photoswitch 3,3′-bis(sulfonato)-4,4′-bis(chloroacetamido)azobenzene (BSBCA) was subsequently covalently linked to the cysteine residues, as described earlier.[61,84] The successful linkage, purity, as well as the integrity of the peptide, was controlled via mass spectrometry.

B. Protein preparation

Human MCL-1 (hMCL-1ΔN-ΔC, 171-327, C286S[85]) was expressed in *Escherichia coli* BL21. The cells were grown until they reached OD_{600} = 0.6 and induced with 0.75 mM isopropyl β-D-1-thiogalactopyranoside. After the induction, the cells were incubated for 20 h at 30 °C until they were harvested end lysed using sonication. The proteins were purified under native conditions via Ni-affinity chromatography and a His_6-Tag at the N-terminus of the protein. The N-terminal His_6-Tag was removed by 3C protease cleavage. All experiments were performed in 50 mM Tris (pH 8) and 125 mM NaCl. The integrity, as well as the purity of the protein sample, was controlled via mass spectrometry. For IR spectroscopy, H_2O containing sample buffer was exchanged against D_2O based buffer via spin column centrifugation. To circumvent the contamination with atmospheric H_2O, the sample was kept in a water-vapor free nitrogen environment.

C. Transient IR spectroscopy

For pump–probe measurements, we used two electronically synchronized 2.5 kHz Ti:sapphire oscillator/regenerative amplifier femtosecond laser systems (Spectra Physics), allowing a delay of maximally 45 μs.[86] For the pump pulses, one laser system was tuned to 840 nm and then brought to 420 nm pulses via second harmonic generation in a β-BaBO$_4$ crystal, later needed for *cis*-to-*trans*-isomerization of the photoswitch. After light amplification, the compressor has been bypassed, resulting in ≈60 ps stretched pulses, in order to reduce sample deposition on the sample cell windows. At the sample cell, the power was 3 μJ per pulse, focused to a ≈140 μm beam diameter. The second laser system was used to generate mid-IR probe pulses in an optical parametric amplifier (100 fs, spot size 110 μm, center wavenumber 1625 cm^{-1}).[87] To prepare the investigated samples for the spectroscopic experiments, the crosslinked peptides and MCL-1 were mixed in a 1:1 ratio in D_2O with a total complex concentration of 1 mM. The protein samples were constantly circulated in a closed-cycle flow cell system, comprising a CaF$_2$ measurement cell (50 μm optical path length) and a reservoir. The measurement took place for 2 to 3 h at room temperature. The

sample was visually controlled for degradation on the CaF$_2$ windows. To exclude precipitated protein from the measurement, the sample was centrifuged before every experiment and the supernatant was used. To prepare the investigated sample for the measurement in the *cis*-state, we irradiated it with a 375 nm continuous wave diode laser (90 mW, CrystaLaser) before entering the measurement cell. This guaranteed that the sample was >85% in *cis*-state.[84] In the past, it was shown that azobenzene photoswitches had photoisomerization quantum yields that were substantially higher for *cis*-to-*trans* switching than for *trans*-to-*cis*. Furthermore, this was demonstrated to be independent of the bound peptide.[88] Thus, *trans*-switched peptides are in a minority and additionally exhibit a lower isomerization quantum yield than their *cis*-counterparts, resulting in a negligibly small effect on the effective signal upon *cis*-to-*trans* photoswitching.

D. Peptide parameter computation

To better understand the differences of the various BH3-only peptides, we calculated parameters for the polarity according to Grantham,[68] and the hydrophobicity/hydropathicity according to Kyte and Doolittle[69] from the sequences of PUMA, BIM, and NOXA using the Expasy/ProtScale server (http://web.expasy.org/protscale/). The calculations were executed with a window size of seven residues (interval length for the computation) and the same weight for every residue in that interval (relative weight = 100%).[89] The Kyte–Doolittle method was used here explicitly with a window size of seven that allows the scan for hydrophobic/hydrophilic regions.[89] On the resulting hydropathicity scale, positive values indicate hydrophobic and negative values hydrophilic regions.

SUPPLEMENTARY MATERIAL

See the supplementary material for steady-state IR difference spectra of isolated PUMA and NOXA.

NOMENCLATURE

BH	BCL-2 homology
BSBCA	3,3′-bis(sulfonato)-4,4′-bis-(chloroacetamido) azobenzene
CD	Circular dichroism
EADS	evolution associated difference spectra
IR	Infrared
MCL-1	Myeloid cell leukemia 1.

AUTHOR DECLARATIONS

Conflict of Interest

The authors have no conflicts to disclose.

Author Contributions

Philipp J. Heckmeier: Conceptualization (lead); Investigation (lead); Software (supporting); Visualization (lead); Writing – original draft (equal). **Jeannette Ruf**: Investigation (supporting); Software (supporting). **Brankica G. Janković**: Conceptualization (supporting). **Peter Hamm**: Funding acquisition (lead); Resources (lead); Software (lead); Supervision (lead); Writing – original draft (equal).

DATA AVAILABILITY

The data that support the findings of this study are openly available in Zenodo at https://doi.org/10.5281/zenodo.7561735, Ref. 90.

REFERENCES

[1] H. Jeong, S. P. Mason, A.-L. Barabási, and Z. N. Oltvai, "Lethality and centrality in protein networks," Nature **411**, 41 (2001).

[2] L. H. Hartwell, J. J. Hopfield, S. Leibler, and A. W. Murray, "From molecular to modular cell biology," Nature **402**, C47 (1999).

[3] Z. Jin and W. S. El-Deiry, "Overview of cell death signaling pathways," Cancer Biol. Ther. **4**, 147 (2005).

[4] C.-J. Tsai, S. Kumar, B. Ma, and R. Nussinov, "Folding funnels, binding funnels, and protein function," Protein Sci. **8**, 1181 (1999).

[5] K. Sugase, H. J. Dyson, and P. E. Wright, "Mechanism of coupled folding and binding of an intrinsically disordered protein," Nature **447**, 1021 (2007).

[6] P. E. Wright and H. J. Dyson, "Linking folding and binding," Curr. Opin. Struct. Biol. **19**, 31 (2009).

[7] S. Kumar, B. Ma, C.-J. Tsai, N. Sinha, and R. Nussinov, "Folding and binding cascades: Dynamic landscapes and population shifts," Protein Sci. **9**, 10 (2000).

[8] D. D. Boehr, R. Nussinov, and P. E. Wright, "The role of dynamic conformational ensembles in biomolecular recognition," Nat. Chem. Biol. **5**, 789 (2009).

[9] D. E. Koshland, "Application of a theory of enzyme specificity to protein synthesis," Proc. Natl. Acad. Sci. U. S. A. **44**, 98 (1958).

[10] P. Csermely, R. Palotai, and R. Nussinov, "Induced fit, conformational selection and independent dynamic segments: An extended view of binding events," Trends Biochem. Sci. **35**, 539 (2010).

[11] A. K. Dunker, M. S. Cortese, P. Romero, L. M. Iakoucheva, and V. N. Uversky, "Flexible nets: The roles of intrinsic disorder in protein interaction networks," FEBS J. **272**, 5129 (2005).

[12] P. M. Kim, A. Sboner, Y. Xia, and M. Gerstein, "The role of disorder in interaction networks: A structural analysis," Mol. Syst. Biol. **4**, 179 (2008).

[13] V. N. Uversky, "Unusual biophysics of intrinsically disordered proteins," Biochim. Biophys. Acta Proteins Proteom. **1834**, 932 (2013).

[14] R. J. Youle and A. Strasser, "The BCL-2 protein family: Opposing activities that mediate cell death," Nat. Rev. Mol. Cell Biol. **9**, 47 (2008).

[15] J. Kale, E. J. Osterlund, and D. W. Andrews, "BCL-2 family proteins: Changing partners in the dance towards death," Cell Death Differ. **25**, 65 (2018).

[16] M. G. Hinds, C. Smits, R. Fredericks-Short, J. M. Risk, M. Bailey, D. C. S. Huang, and C. L. Day, "Bim, Bad and Bmf: Intrinsically unstructured BH3-only proteins that undergo a localized conformational change upon binding to prosurvival Bcl-2 targets," Cell Death Differ. **14**, 128 (2007).

[17] L. Dahal, T. O. C. Kwan, J. J. Hollins, and J. Clarke, "Promiscuous and selective: How intrinsically disordered BH3 proteins interact with their pro-survival partner MCL-1," J. Mol. Biol. **430**, 2468 (2018).

[18] J. M. Adams and S. Cory, "The Bcl-2 apoptotic switch in cancer development and therapy," Oncogene **26**, 1324 (2007).

[19] P. E. Czabotar, G. Lessene, A. Strasser, and J. M. Adams, "Control of apoptosis by the BCL-2 protein family: Implications for physiology and therapy," Nat. Rev. Mol. Cell Biol. **15**, 49 (2014).

[20] R. Roufayel, K. Younes, A. Al-Sabi, and N. Murshid, "BH3-only proteins NOXA and PUMA are key regulators of induced apoptosis," Life **12**, 256 (2022).

[21] A. Bolomsky, M. Vogler, M. C. Köse, C. A. Heckman, G. Ehx, H. Ludwig, and J. Caers, "MCL-1 inhibitors, fast-lane development of a new class of anti-cancer agents," J. Hematol. Oncol. **13**, 173 (2020).

[22] L. W. Thomas, C. Lam, and S. W. Edwards, "Mcl-1; the molecular regulation of protein function," FEBS Lett. **584**, 2981 (2010).

[23] R. W. Craig, "MCL1 provides a window on the role of the BCL2 family in cell proliferation, differentiation and tumorigenesis," Leukemia **16**, 444 (2002).

[24] S. Fletcher, "MCL-1 inhibitors-where are we now (2019)?," Expert Opin. Ther. Pat. **29**, 909 (2019).

[25] T. L. Bonneaud, C. C. Lefebvre, L. Nocquet, A. Basseville, J. Roul, H. Weber, M. Campone, P. P. Juin, and F. Souazé, "Targeting of MCL-1 in breast cancer-associated fibroblasts reverses their myofibroblastic phenotype and pro-invasive properties," Cell Death Dis. **13**, 787 (2022).

[26] S. Lee, T. E. Wales, S. Escudero, D. T. Cohen, J. Luccarelli, C. G. Gallagher, N. A. Cohen, A. J. Huhn, G. H. Bird, J. R. Engen, and L. D. Walensky, "Allosteric inhibition of antiapoptotic MCL-1," Nat. Struct. Mol. Biol. **23**, 600 (2016).

[27] M. Benabderrahmane, R. Bureau, A. S. Voisin-Chiret, and J. Sopkova-De Oliveira Santos, "Insights into Mcl-1 conformational states and allosteric inhibition mechanism from molecular dynamics simulations, enhanced sampling, and pocket crosstalk analysis," J. Chem. Inf. Model. **60**, 3172 (2020).

[28] P. E. Czabotar, E. F. Lee, M. F. van Delft, C. L. Day, B. J. Smith, D. C. S. Huang, W. D. Fairlie, M. G. Hinds, and P. M. Colman, "Structural insights into the degradation of Mcl-1 induced by BH3 domains," Proc. Natl. Acad. Sci. U. S. A. **104**, 6217 (2007).

[29] C. L. Day, C. Smits, F. C. Fan, E. F. Lee, W. D. Fairlie, and M. G. Hinds, "Structure of the BH3 domains from the p53-inducible BH3-only proteins noxa and puma in complex with Mcl-1," J. Mol. Biol. **380**, 958 (2008).

[30] J. A. Miles, D. J. Yeo, P. Rowell, S. Rodriguez-Marin, C. M. Pask, S. L. Warriner, T. A. Edwards, and A. J. Wilson, "Hydrocarbon constrained peptides – understanding preorganisation and binding affinity," Chem. Sci. **7**, 3694 (2016).

[31] J. M. Rogers, A. Steward, and J. Clarke, "Folding and binding of an intrinsically disordered protein: Fast, but not 'diffusion-limited,'" J. Am. Chem. Soc. **135**, 1415 (2013).

[32] J. M. Rogers, C. T. Wong, and J. Clarke, "Coupled folding and binding of the disordered protein PUMA does not require particular residual structure," J. Am. Chem. Soc. **136**, 5197 (2014).

[33] J. M. Rogers, V. Oleinikovas, S. L. Shammas, C. T. Wong, D. De Sancho, C. M. Baker, and J. Clarke, "Interplay between partner and ligand facilitates the folding and binding of an intrinsically disordered protein," Proc. Natl. Acad. Sci. U. S. A. **111**, 15420 (2014).

[34] P. J. Heckmeier, J. Ruf, D. Buhrke, B. G. Janković, and P. Hamm, "Signal propagation within the MCL-1/BIM protein complex," J. Mol. Biol. **434**, 167499 (2022).

[35] Y. Mei, W. Du, Y. Yang, and M. Wu, "Puma*Mcl-1 interaction is not sufficient to prevent rapid degradation of Mcl-1," Oncogene **24**, 7224 (2005).

[36] S. N. Willis, L. Chen, G. Dewson, A. Wei, E. Naik, J. I. Fletcher, J. M. Adams, and D. C. S. Huang, "Proapoptotic Bak is sequestered by Mcl-1 and Bcl-xL, but not Bcl-2, until displaced by BH3-only proteins," Genes Dev. **19**, 1294 (2005).

[37] V. Sora and E. Papaleo, "Structural details of BH3 motifs and BH3-mediated interactions: An updated perspective," Front. Mol. Biosci. **9**, 1 (2022).

[38] S. Kumar, B. Ma, C.-J. Tsai, H. Wolfson, and R. Nussinov, "Folding funnels and conformational transitions via hinge-bending motions," Cell Biochem. Biophys. **31**, 141 (1999).

[39] C.-J. Tsai, B. Ma, and R. Nussinov, "Folding and binding cascades: Shifts in energy landscapes," Proc. Natl. Acad. Sci. U. S. A. **96**, 9970 (1999).

[40] H. Y. Aviram, M. Pirchi, H. Mazal, Y. Barak, I. Riven, and G. Haran, "Direct observation of ultrafast large-scale dynamics of an enzyme under turnover conditions," Proc. Natl. Acad. Sci. U. S. A. **115**, 3243 (2018).

[41] A. Borgia, M. B. Borgia, K. Bugge, V. M. Kissling, P. O. Heidarsson, C. B. Fernandes, A. Sottini, A. Soranno, K. J. Buholzer, D. Nettels, B. B. Kragelund, R. B. Best, and B. Schuler, "Extreme disorder in an ultrahigh-affinity protein complex," Nature **555**, 61 (2018).

[42] M. Kovermann, C. Grundström, A. E. Sauer-Eriksson, U. H. Sauer, and M. Wolf-Watz, "Structural basis for ligand binding to an enzyme by a conformational selection pathway," Proc. Natl. Acad. Sci. U. S. A. **114**, 6298 (2017).

[43] O. F. Lange, N.-A. Lakomek, C. Farès, G. F. Schröder, K. F. A. Walter, S. Becker, J. Meiler, H. Grubmüller, C. Griesinger, and B. L. De Groot, "Recognition dynamics up to microseconds revealed from an RDC-derived ubiquitin ensemble in solution," Science **320**, 1471 (2008).

[44] B. Buchli, S. A. Waldauer, R. Walser, M. L. Donten, R. Pfister, N. Blöchliger, S. Steiner, A. Caflisch, O. Zerbe, and P. Hamm, "Kinetic response of a photoperturbed allosteric protein," Proc. Natl. Acad. Sci. U. S. A. **110**, 11725 (2013).

[45] B. Jankovic, J. Ruf, C. Zanobini, O. Bozovic, D. Buhrke, and P. Hamm, "Sequence of events during peptide unbinding from RNase S: A complete experimental description," J. Phys. Chem. Lett. **12**, 5201 (2021).

[46] A. Barth, "Infrared spectroscopy of proteins," Biochim. Biophys. Acta, Bioenerg. **1767**, 1073 (2007).

[47] V. A. Lórenz-Fonfría, "Infrared difference spectroscopy of proteins: From bands to bonds," Chem. Rev. **120**, 3466 (2020).

[48] K. Gerwert, G. Souvignier, and B. Hess, "Simultaneous monitoring of light-induced changes in protein side-group protonation, chromophore isomerization, and backbone motion of bacteriorhodopsin by time-resolved Fourier-transform infrared spectroscopy," Proc. Natl. Acad. Sci. U. S. A. **87**, 9774 (1990).

[49] D. Buhrke, K. T. Oppelt, P. J. Heckmeier, R. Fernández-Terán, and P. Hamm, "Nanosecond protein dynamics in a red/green cyanobacteriochrome revealed by transient IR spectroscopy," J. Chem. Phys. **153**, 245101 (2020).

[50] D. Buhrke, N. Michael, and P. Hamm, "Vibrational couplings between protein and cofactor in bacterial phytochrome Agp1 revealed by 2D-IR spectroscopy," Proc. Natl. Acad. Sci. U. S. A. **119**, e2206400119 (2022).

[51] V. A. Lórenz-Fonfría, T. Resler, N. Krause, M. Nack, M. Gossing, G. F. Von Mollard, C. Bamann, E. Bamberg, R. Schlesinger, and J. Heberle, "Transient protonation changes in channelrhodopsin-2 and their relevance to channel gating," Proc. Natl. Acad. Sci. U. S. A. **110**, E1273 (2013).

[52] S. P. Laptenok, A. A. Gil, C. R. Hall, A. Lukacs, J. N. Iuliano, G. A. Jones, G. M. Greetham, P. Donaldson, A. Miyawaki, P. J. Tonge, and S. R. Meech, "Infrared spectroscopy reveals multi-step multi-timescale photoactivation in the photoconvertible protein archetype dronpa," Nat. Chem. **10**, 845 (2018).

[53] J. T. Kennis and M.-L. Groot, "Ultrafast spectroscopy of biological photoreceptors," Curr. Opin. Struct. Biol. **17**, 623 (2007).

[54] T. Kottke, V. A. Lórenz-Fonfría, and J. Heberle, "The grateful infrared: Sequential protein structural changes resolved by infrared difference spectroscopy," J. Phys. Chem. A **121**, 335 (2017).

[55] J. R. Kumita, O. S. Smart, and G. A. Woolley, "Photo-control of helix content in a short peptide," Proc. Natl. Acad. Sci. U. S. A. **97**, 3803 (2000).

[56] J. A. Ihalainen, J. Bredenbeck, R. Pfister, J. Helbing, L. Chi, I. H. M. Van Stokkum, G. A. Woolley, and P. Hamm, "Folding and unfolding of a photoswitchable peptide from picoseconds to microseconds," Proc. Natl. Acad. Sci. U. S. A. **104**, 5383 (2007).

[57] J. Wachtveitl, S. Spörlein, H. Satzger, B. Fonrobert, C. Renner, R. Behrendt, D. Oesterhelt, L. Moroder, and W. Zinth, "Ultrafast conformational dynamics in cyclic azobenzene peptides of increased flexibility," Biophys. J. **86**, P2350 (2004).

[58] M. S. Rampp, S. M. Hofmann, T. Podewin, A. Hoffmann-Röder, L. Moroder, and W. Zinth, "Time-resolved infrared studies of the unfolding of a light triggered β-hairpin peptide," Chem. Phys. **512**, 116 (2018).

[59] O. Bozovic, C. Zanobini, A. Gulzar, B. Jankovic, D. Buhrke, M. Post, S. Wolf, G. Stock, and P. Hamm, "Real-time observation of ligand-induced allosteric transitions in a PDZ domain," Proc. Natl. Acad. Sci. U. S. A. **117**, 26031 (2020).

[60] N. London, S. Gullá, A. E. Keating, and O. Schueler-Furman, "In *silico* and *in vitro* elucidation of BH3 binding specificity toward Bcl-2," Biochemistry **51**, 5841 (2012).

[61] Z. Zhang, D. C. Burns, J. R. Kumita, O. S. Smart, and G. A. Woolley, "A water-soluble azobenzene cross-linker for photocontrol of peptide conformation," Bioconjugate Chem. **14**, 824 (2003).

[62] A. Barth and C. Zscherp, "What vibrations tell us about proteins," Q. Rev. Biophys. **35**, 369 (2002).

[63] M. P. Hobson and A. N. Lasenby, "The entropic prior for distributions with positive and negative values," Mon. Not. R. Astron. Soc. **298**, 905 (1998).

[64] A. T. N. Kumar, L. Zhu, J. F. Christian, A. A. Demidov, and P. M. Champion, "On the rate distribution analysis of kinetic data using the maximum entropy method: Applications to myoglobin relaxation on the nanosecond and femtosecond timescales," J. Phys. Chem. B **105**, 7847 (2001).

[65] V. A. Lórenz-Fonfría and H. Kandori, "Transformation of time-resolved spectra to lifetime-resolved spectra by maximum entropy inversion of the laplace transform," Appl. Spectrosc. **60**, 407 (2006).

[66] I. H. M. Van Stokkum, D. S. Larsen, and R. Van Grondelle, "Global and target analysis of time-resolved spectra," Biochim. Biophys. Acta, Bioenerg. **1657**, 82 (2004).

[67] C.-Y. Huang, Z. Getahun, Y. Zhu, J. W. Klemke, W. F. Degrado, and F. Gai, "Helix formation via conformation diffusion search," Proc. Natl. Acad. Sci. U. S. A. **99**, 2788 (2002).

[68] R. Grantham, "Amino acid difference formula to help explain protein evolution," Science **185**, 862 (1974).

[69] J. Kyte and R. F. Doolittle, "A simple method for displaying the hydropathic character of a protein," J. Mol. Biol. **157**, 105 (1982).

[70] Y. Chebaro, A. J. Ballard, D. Chakraborty, and D. J. Wales, "Intrinsically disordered energy landscapes," Sci. Rep. **5**, 10386 (2015).

[71] W. T. Chu, J. Clarke, S. L. Shammas, and J. Wang, "Role of non-native electrostatic interactions in the coupled folding and binding of PUMA with Mcl-1," PLoS Comput. Biol. **13**, e1005468 (2017).

[72] M. L. Stewart, E. Fire, A. E. Keating, and L. D. Walensky, "The MCL-1 BH3 helix is an exclusive MCL-1 inhibitor and apoptosis sensitizer," Nat. Chem. Biol. **6**, 595 (2010).

[73] X. Pang, J. Zhang, H. Lopez, Y. Wang, W. Li, K. L. O'Neill, J. J. D. Evans, N. M. George, J. Long, Y. Chen, and X. Luo, "The carboxyl-terminal tail of Noxa protein regulates the stability of Noxa and Mcl-1," J. Biol. Chem. **289**, 17802 (2014).

[74] K. P. Murphy and E. Freire, *Thermodynamics of Structural Stability and Cooperative Folding Behavior in Proteins* (Academic Press, 1992), pp. 313–361.

[75] J. M. Matthews, "Plasticity at protein–protein interaction interfaces," in *Encyclopedia of Biophysics*, edited by G. C. K. Roberts (Springer, Berlin, Heidelberg, 2013), pp. 1886–1888.

[76] C. N. Pace, B. A. Shirley, M. McNutt, and K. Gajiwala, "Forces contributing to the conformational stability of proteins," FASEB J. **10**, 75 (1996).

[77] R. Guerois, J. E. Nielsen, and L. Serrano, "Predicting changes in the stability of proteins and protein complexes: A study of more than 1000 mutations," J. Mol. Biol. **320**, 369 (2002).

[78] M. Majewski, S. Ruiz-Carmona, and X. Barril, "An investigation of structural stability in protein-ligand complexes reveals the balance between order and disorder," Commun. Chem. **2**, 110 (2019).

[79] C. Smits, P. E. Czabotar, M. G. Hinds, and C. L. Day, "Structural plasticity underpins promiscuous binding of the prosurvival protein A1," Structure **16**, 818 (2008).

[80] T. L. Tapley, J. L. Körner, M. T. Barge, J. Hupfeld, J. A. Schauerte, A. Gafni, U. Jakob, and J. C. A. Bardwell, "Structural plasticity of an acid-activated chaperone allows promiscuous substrate binding," Proc. Natl. Acad. Sci. U. S. A. **106**, 5557 (2009).

[81] A. E. Ashcroft, A. Brinker, J. E. Coyle, F. Weber, M. Kaiser, L. Moroder, M. R. Parsons, J. Jager, U. F. Hartl, M. Hayer-Hartl, and S. E. Radford, "Structural plasticity and noncovalent substrate binding in the GroEL apical domain. A study using electrospray ionization mass spectrometry and fluorescence binding studies," J. Biol. Chem. **277**, 33115 (2002).

[82] N. Plattner and F. Noé, "Protein conformational plasticity and complex ligand-binding kinetics explored by atomistic simulations and Markov models," Nat. Commun. **6**, 7653 (2015).

[83] M. Huse and J. Kuriyan, "The conformational plasticity of protein kinases," Cell **109**, 275 (2002).

16 January 2024 11:26:02

[84]B. Jankovic, A. Gulzar, C. Zanobini, O. Bozovic, S. Wolf, G. Stock, and P. Hamm, "Photocontrolling protein–peptide interactions: From minimal perturbation to complete unbinding," J. Am. Chem. Soc. **141**, 10702 (2019).

[85]G. Liu, L. Poppe, K. Aoki, H. Yamane, J. Lewis, and T. Szyperski, "High-quality NMR structure of human anti-apoptotic protein domain Mcl-1(171-327) for cancer drug design," PLoS One **9**, e96521 (2014).

[86]J. Bredenbeck, J. Helbing, and P. Hamm, "Continuous scanning from picoseconds to microseconds in time resolved linear and nonlinear spectroscopy," Rev. Sci. Instrum. **75**, 4462 (2004).

[87]P. Hamm, R. A. Kaindl, and J. Stenger, "Noise suppression in femtosecond mid-infrared light sources," Opt. Lett. **25**, 1798 (2000).

[88]V. Borisenko and G. A. Woolley, "Reversibility of conformational switching in light-sensitive peptides," J. Photochem. Photobiol., A **173**, 21 (2005).

[89]E. Gasteiger, C. Hoogland, A. Gattiker, S. Duvaud, M. R. Wilkins, R. D. Appel, and A. Bairoch, "Protein identification and analysis tools on the ExPASy server," in *The Proteomics Protocols Handbook*, edited by J. M. Walker (Humana Press, Totowa, NJ, 2005) pp. 571–607.

[90]P. J. Heckmeier (2023). "MCL-1 promiscuity and the structural resilience of its binding partners – DATA," Zenodo. https://doi.org/10.5281/zenodo.7561735

16 January 2024 11:26:02